

JET-INDUCED FLOW IN CYLINDRICAL TANKS II. NUMERICAL SOLUTION

I. TUWEGIAR and Elemér LITVAI

Department of Fluid Dynamics
Technical University of Budapest
H-1521 Budapest, Hungary

Received: December 10, 1996

Abstract

In part I, a model for the jet-induced flow in cylindrical tanks based on flow visualization and measurements has been delineated. In this part, the model is formally formulated and solved. A Coupled Block Line Newton-Gauss-Seidel method is used to linearize and solve the resulting equations. The method was found efficient and robust with possibility of overrelaxation. It also provides for introducing higher order schemes in a simple manner.

Keywords: angularly averaged cylindrical symmetry, prescribed tangential velocity, Newton-type linearization, coupling of variables, faster convergence, overrelaxation.

1. Introduction

In part I, we have conducted a visualization study to understand the nature of the flow and carried out measurements of the tangential velocity on the free surface. A mathematical model for predicting its distribution on the free surface was deduced from the Navier-Stokes equations and verified by comparison to experimental data. In this part we use these findings to formulate a complete mathematical model to predict the flow field in the whole tank. The model is solved numerically by linearizing the algebraic equations using Newton's linearization.

No work on the same problem was encountered in the available literature. However, works on problems with cylindrical geometry were useful in the development of the numerical procedure and the testing of the computer program. The investigation of laminar flow in cylindrical containers driven by rotating end or side walls is famous. It is an idealization used in attempts to understand the forces that cause and maintain such atmospheric phenomena as tornadoes and dust whirls. TEXTER et al. [13] and HSIEN [10] made early attempts to obtain a numerical solution for this problem with application to a conceptual nuclear design. They solved stream function-vorticity-circulation set of equations using iterative methods. Heavy underrelaxation was necessary even for small Reynolds numbers. The author faced similar problems when attempted to use iterative methods to save on computer storage [14]. Improved methods revealed the fine details of

flow at high Reynolds numbers [1, 8, 11]. He treated the free surface as a free shear boundary. Mechanical mixing of chemical vessels is another application where useful experience may be found. HARVEY and GREAVES [3] solved turbulent flow in agitated vessel using the $k - \varepsilon$ model. They remarked that turbulence in the agitated vessel tends to be homogeneous away from the impeller. Reports on jet mixing are less common. LANE and RICE [6] investigated jet mixing experimentally employing inclined side entry jet. Their interest was in the correlation of mixing times. They reported some characteristics of the submerged bounded jet [7] and gave correlation for the entrainment rate of the jet. They concluded that the flow is totally turbulent at a jet Reynolds number larger than 2000. Their finding may be useful in formulating the boundary condition of the jet in our case if full three dimensional calculations are desirable. A review of jet mixing before 1986 is found in [5]. A third important application from which we may draw some experience is the vortex combustor. The geometry is usually cylindrical. Local three-dimensional flow exists near the air injection ports but the flow is treated as axisymmetric [9]. Several other useful works in different fields are available. See for example references [12, 17, 18].

2. The Mathematical Model

The distribution of the tangential velocity on the free surface which has been confirmed by experiment is used as a boundary condition for the axisymmetric Navier-Stokes equations in cylindrical coordinates. The $\omega - \psi - \Gamma$ is given by:

$$\frac{\partial}{\partial X_1} \left(\frac{N}{M} \frac{1}{R} \frac{\partial \Psi}{\partial X_1} \right) + \frac{\partial}{\partial X_2} \left(\frac{M}{N} \frac{1}{R} \frac{\partial \Psi}{\partial X_2} \right) + \frac{\Omega}{NM} = 0, \quad (1)$$

$$R^2 \left[\frac{\partial}{\partial X_1} \left(\frac{\Omega}{R} \frac{\partial \Psi}{\partial X_2} \right) - \frac{\partial}{\partial X_2} \left(\frac{\Omega}{R} \frac{\partial \Psi}{\partial X_1} \right) \right] - \frac{\partial}{\partial X_1} \left(\frac{N}{M} R^3 \frac{\partial}{\partial X_1} \left(\frac{\Omega}{R} \right) \right) - \frac{\partial}{\partial X_2} \left(\frac{M}{N} R^3 \frac{\partial}{\partial X_2} \left(\frac{\Omega}{R} \right) \right) + \frac{1}{M} \frac{1}{R^2} \frac{\partial \Gamma^2}{\partial X_1} = 0. \quad (2)$$

$$\left[\frac{\partial}{\partial X_1} \left(\Gamma \frac{\partial \Psi}{\partial X_2} \right) - \frac{\partial}{\partial X_2} \left(\Gamma \frac{\partial \Psi}{\partial X_1} \right) \right] - \frac{\partial}{\partial X_1} \left\{ \frac{N}{M} R^3 \frac{\partial}{\partial X_1} \left(\frac{\Gamma}{R^2} \right) \right\} - \frac{\partial}{\partial X_2} \left\{ \frac{M}{N} R^3 \frac{\partial}{\partial X_2} \left(\frac{\Gamma}{R^2} \right) \right\} = 0. \quad (3)$$

2.1. Boundary Conditions

Eqs (1 - 3) are made unique to the studied case by imposing the boundary conditions:

2.2. Free Surface

At the free surface, the tangential velocity distribution derived in part I is used

$$V_{\theta} = \frac{V_{\theta 2} r_2}{1 - e^{-\lambda/2}} \frac{(1 - e^{-(\lambda/2)R^2})}{r}. \quad (4)$$

$\lambda = 8$ and formula for calculating $V_{\theta 2}$ was given in part I. This boundary condition is an important part of the proposed model since it accounts for the effect of the jet on average basis. The free surface is assumed to be flat since the ratio of centrifugal forces to gravitational forces (Froud's number) is much smaller than one [4].

2.3. Walls

At walls we used wall functions to bridge the steep gradients of velocity near the wall (see [15] for details).

2.4. Axis of Symmetry

At the axis of symmetry the stream function and the circulation are zero. The vorticity is calculated from:

$$\left(\frac{\omega}{r}\right)_1 = 8 \left[\frac{\frac{\psi_3 - \psi_1}{X_{2,3}^2} \frac{\psi_2 - \psi_1}{X_{2,2}^2}}{X_{2,2}^2 - X_{2,3}^2} \right]. \quad (5)$$

Subscript 1 stands for the axis and 2 and 3 for adjacent points.

3. Numerical Solution

Eqs (1 - 3) were integrated by the control volume method (Fig. 1) the resulting discrete equation having been written as:

$$A_P \varphi_P = A_E \varphi_E + A_W \varphi_W + A_N \varphi_N + A_S \varphi_S + S_u, \quad (5a)$$

with φ standing for ψ , Ω or Γ respectively.

First, Eq. (5a) was solved by conventional alternating line sweeps. Then, a more robust and efficient method based on Newton's linearization is formulated [14, 15, 16].

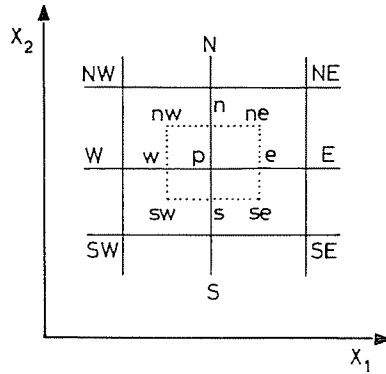


Fig. 1. Grid

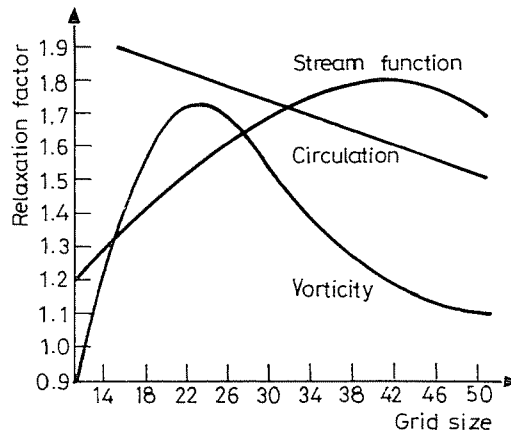


Fig. 2. Optimal relaxation factors for NM

4. The Couple Block Line Newton–Gauss–Seidel Scheme (CBLNGS)

Eqs (1 – 3) are written in the form:

$$R_v^{n+1}(\psi, \omega, \Gamma) = 0, \quad R_\omega^{n+1}(\psi, \omega, \Gamma) = 0 \quad \text{and} \quad R_\Gamma^{n+1}(\psi, \omega, \Gamma) = 0, \quad (6)$$

where n denotes the iteration number. Expansion of the residuals over an

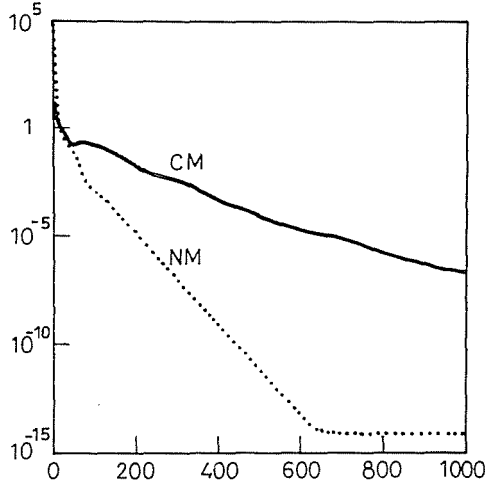


Fig. 3. Residual reduction rate for *CM* and *NM* on 31×31 grid

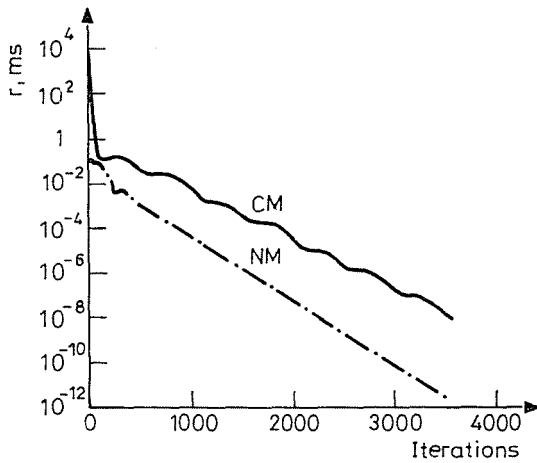


Fig. 4. Residual reduction rate for *CM* and *NM* on 51×51 grid

iteration step yields:

$$R_{\psi}^{n+1} = R_{\psi}^n + \frac{\partial R_{\psi}}{\partial \psi} \Delta \psi^{n+1} + \frac{\partial R_{\psi}}{\partial \omega} \Delta \omega^{n+1} + \frac{\partial R_{\psi}}{\partial \Gamma} \Delta \Gamma^{n+1} = 0, \quad (7)$$

here $\Delta \psi^{n+1} = \psi^{n+1} - \psi^n$ and similar expression for ω and Γ . Higher-order terms have been neglected. Eq. (6) is a set of linear algebraic equations for the corrections. When the unknowns are strongly coupled in one direction, they have to be relaxed simultaneously. By extending the linearization to the neighboring points along a line and solve for the unknowns lying on that

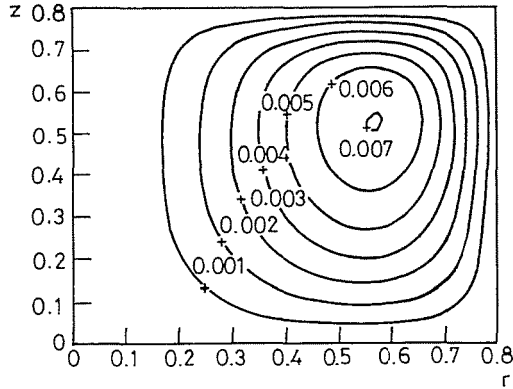


Fig. 5. Contours of stream function (51×51)

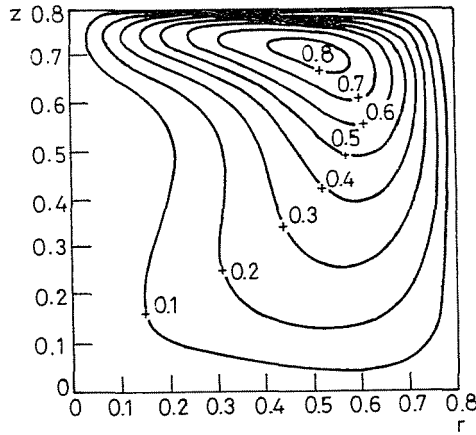


Fig. 6. Lines of constant vorticity (51×51)

line simultaneously we obtain the Coupled Block Line Newton–Gauss–Seidel (CBLNGS) scheme.

5. Solution Procedure

Eq. (6) can be written in the general Newton form :

$$J\Delta\Phi = -R, \quad (8)$$

where J is the Jacobian, $\Delta\Phi$ is the correction vector and R is the residual vector. The corrections obtained by solving Eq. (7) are applied to the unknowns as follows :

$$\psi_p^{n+1} = \psi_p^n + \varepsilon_\psi \Delta\psi_p, \quad (9)$$

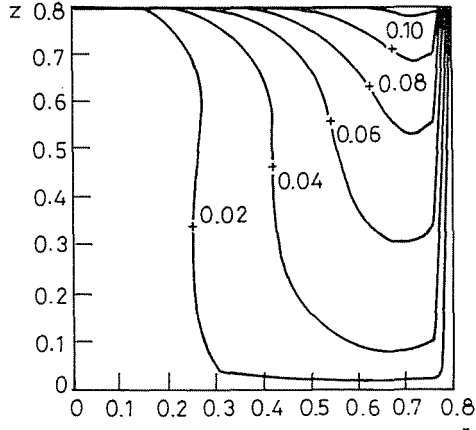


Fig. 7. Lines of constant circulation (51×51)

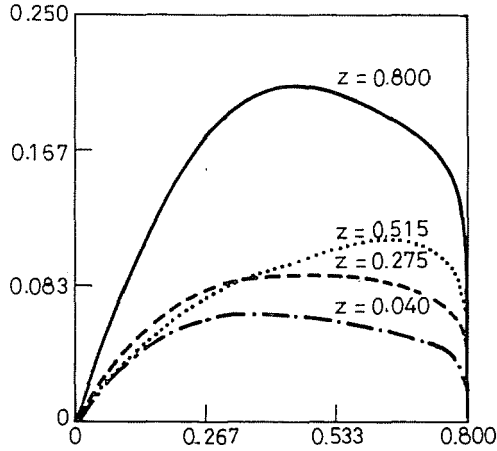


Fig. 8. Distribution of tangential velocity at various heights

$$\omega_p^{n+1} = \omega_p^n + \varepsilon_\omega \Delta\omega_p, \tag{10}$$

$$\Gamma_p^{n+1} = \Gamma_p^n + \varepsilon_\Gamma \Delta\Gamma_p, \tag{11}$$

where n is the iteration number and ε is a relaxation parameter. When $\varepsilon < 1$ the corrections are damped or underrelaxed. For $\varepsilon > 1$ we have overrelaxation.

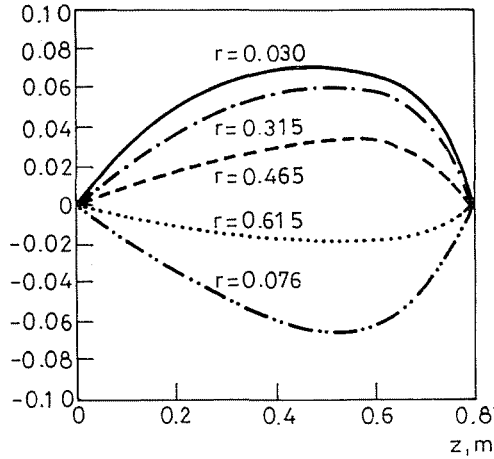


Fig. 9. Distribution of the axial velocity for various radial locations

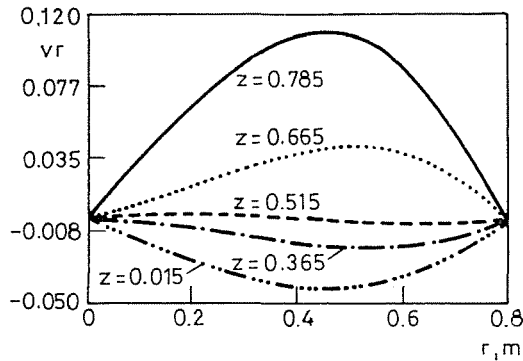


Fig. 10. Distribution of the radial velocity

6. Introducing Higher Order Difference Schemes

At convergence, the residuals diminish. The accuracy of the numerical solution, therefore, depends on the accuracy of the discretization of the right hand side of Eq. (7). The form of the Jacobian matrix may affect the convergence rate but not the accuracy of the final solution. In addition, the discretization of the residuals does not have to be stable. For example, one may use central differences for the evaluation of the residuals and FOU scheme for the Jacobian. The latter must be diagonally dominant for convergence.

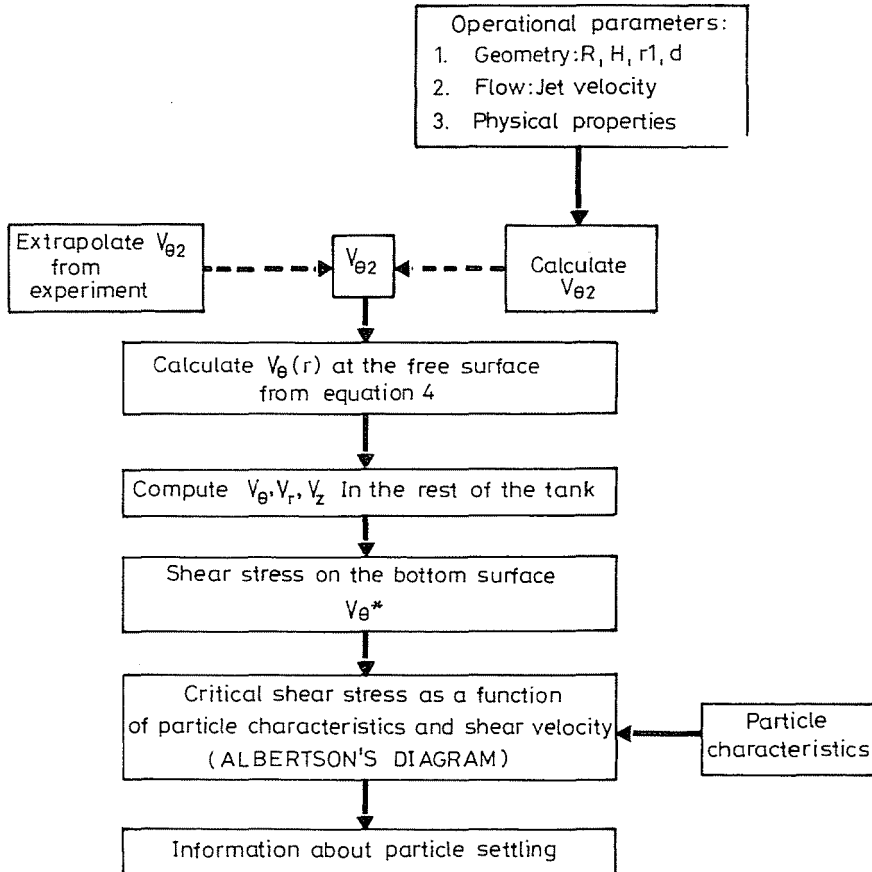


Fig. 11. Solution scheme

7. Results

Fig. 2 shows the dependence of overrelaxation of NM on the number of grid points. This interesting behavior is similar to that found by the author for the Burgers' equations [16]. Figs 3 - 4 display the rate of convergence for the method on 31×31 and 51×51 grids, respectively. The output file from the program allows the plotting of quantities of interest. Figs 5 - 7 show contours of constant stream lines, constant vorticity and constant circulation. Plots of the velocity distribution are given in Figs 8 - 10. Fig. 11 gives a scheme for the solution of the problem. The part concerning the prediction of the onset of the particle movement is not dealt with here (see [15]).

8. Conclusions

In operation and design, simple easy-to-implement methods are desirable. Complex analysis is only needed when safety is an important factor or deep understanding of the phenomena is needed. In addition, for many engineering applications economy is still an overriding factor. The accomplished results comply with these desirable characteristics. A summary of results is

1. The performance of a jet-driven cylindrical mixer can be approximated by modelling the three-dimensional turbulent flow by a cylindrically symmetric, i.e. angularly averaged flow assuming flat surface, constant eddy viscosity and logarithmic velocity profile in the boundary layers near the side and bottom walls.
2. A model for the flow in the whole tank was formulated using the distribution of the tangential velocity on the free surface to account for the effect of the jet. The Navier-Stokes equations in the $\psi - \omega - \Gamma$ form were solved using an alternating line procedure. Solution on 31×31 , 41×41 , and 51×51 grid points showed consistent flow fields characterized by a single secondary vortex drawing settled particles toward the center of the bottom. The convergence slows down as the number of grid points is increased and underrelaxation becomes necessary for higher Reynolds number.
3. A method based on Newton linearization of the discretized equations and the coupling of the variables was formulated and implemented (CBLNGS) and found to be faster and less expensive per iteration than the conventional method. The distinctive features of the implementation are:
 - I. The simple way of incorporation in the existing conventional method.
 - II. The use of block line sweeps.
 - III. The idea of discretization of the residual equation by schemes of higher orders of accuracy. These schemes do not have to be stable.
 - IV. The use of overrelaxation.

References

- [1] DIJKSTRA - VAN HEIJST, G. (1983): The Flow between Two Finite Rotating Disks Enclosed by a Cylinder, *J. Fluid Mech.* Vol. 128, pp. 123-154.
- [2] GOSMAN, A. et al. (1969): Heat and Mass Transfer in Recirculating Flows, Academic Press, London.
- [3] HARVEY, P. - GREAVES, M. (1982): Turbulent Flow in an Agitated Vessel, Part I: A Predictive Model, *Trans IChemE*, Vol. 60.
- [4] HYUN, J. (1985): Flow in an Open Tank with a Free Surface Driven by Spinning Bottom, *J. Fluid Egr.* Vol. 107, p. 495.

- [5] KURODA, C. – OGAWA, K. (1986): Turbulent Swirling Pipe Flow, in The Encyclopedia of Fluid Mechanics, N., P. Chermisiof. Editor, Vol. 6., Gulf Publishing Co.
- [6] LANE, A. – RICE, P. (1982): An Investigation of Liquid Jet Mixing Employing an Inclined Side Entry Jet, *Trans. IChemE*, Vol. 60.
- [7] LANE, A. – RICE, P. (1982): The Flow Characteristics of a Submerged Bounded Jet in a Closed System, *Trans IChemE*, Vol. 60.
- [8] LUGT, H. – ABOUD, M. (1987): Axisymmetric Vortex Breakdown with and without Temperature Effects in a Container with a Rotating Lid, *J. Fluid Mech.* Vol. 179, pp. 179–200.
- [9] NIEH, S. – ZHANG, J. (1992): Simulation of the Strongly Swirling Aerodynamic Field in a Vortex Combustor, *Journal of Fluid Engineering*, Vol. 114.
- [10] HSIEN, P. (1970): A Numerical Computation of a Confined Rotating Flow, *J. Applied Mech.*, June.
- [11] SHAKESPEARE, W. – LEVY, E. (1982): Laminar Boundary Layer Near the Rotating End Wall of a Confined Vortex, *Journal of Fluid Engineering*, June, pp. 171–177.
- [12] STRIKWERDA, J. – NAGEL, Y. (1988): A Numerical Method for the Incompressible Navier-Stokes Equations in Three-Dimensional Cylindrical Geometry, *J. Comp. Phys.*, Vol. 78, pp. 64–78.
- [13] TEXTOR, R. – LICK, D. – FARRIS, G. (1969): Solution of Confined Vortex Problems, *J. Comp. Physics*, Vol. 4, pp. 258.
- [14] TUWEGAR, I. – LITVAI, E. (1993): The Numerical Prediction of Jet Driven Flow in Cylindrical Tanks, *Proceedings of the Eighth Conference on Numerical Methods in Laminar and Turbulent Flow*, Vol. 8, part 1, pp. 118–129, Swansea.
- [15] TUWEGAR, I. (1996): Numerical and Experimental Investigation of Jet-Induced Flow in Cylindrical Tanks, PhD Dissertation, Budapest.
- [16] TUWEGAR, I. (1997): Newton-Relaxation Schemes for Nonlinear Fluid Flow Equations, accepted for publication by the Annals Univ. Sci. Budapest, Sect. Comp.
- [17] VAUGHN, H. – OBERKAMPF, W. -- WOLF, W. (1985): Fluid Motion inside a Spinning Cylinder, *J. Fluid Mech.* Vol. 150, pp. 121–138.
- [18] WILLIAMS, G.: Numerical Integration of the Three-Dimensional Navier-Stokes Equations for Incompressible Flow, *J. Fluid Mech.*, Vol. 37, part 4, pp. 727–750.